

# Thermalization in Krylov Basis

Mohsen Alishahiha<sup>a</sup> and, Mohammad Javad Vasli<sup>b,a</sup>

<sup>a</sup> *School of Physics, Institute for Research in Fundamental Sciences (IPM),  
P.O. Box 19395-5531, Tehran, Iran*

<sup>b</sup> *Department of Physics, University of Guilan,  
P.O. Box 41335-1914, Rasht, Iran*

*E-mails: alishah@ipm.ir , vasli@phd.guilan.ac.ir*

We study thermalization for closed non-integrable quantum systems in the Krylov basis. Following the idea of the eigenstate thermalization hypothesis, one may introduce Krylov basis thermalization hypothesis which imposes a condition on the matrix elements of local operators in the Krylov basis. In this context, the nature of thermalization may be probed by the infinite time average of the Krylov complexity. We also compute the variance of Lanczos coefficients which may provide another quantity to examine the nature of thermalization. We will see that there is a direct relation between the behavior of the infinite time average of complexity and that of the inverse participation ratio of initial states.

## I. INTRODUCTION

Based on our everyday experience, the thermalization of macroscopic systems is one of the most natural phenomena in nature. Although to see a macroscopic system is approaching thermal equilibrium one does not need to produce several copies of the system, the statistical mechanics in which we are dealing with “ensembles” is provided a powerful tool to study thermalization. This has to do with the ergodic property of classical chaotic systems that validates the statistical mechanics. In fact in these systems the ensemble averages used in statistical mechanics calculations agree with the time averages involving in our experiments.

Even though for closed quantum systems one may also observe emerging of the thermal equilibrium in non-equilibrated systems (caused by *e.g.* global quench), unlike the classical systems, the thermalization may be seen without performing any time averages [1, 2]. Indeed, out of equilibrium states approach to their thermal expectations short after relaxation. It is, however, important to note that in closed quantum systems dynamics is unitary and time reversal invariant, and therefore, a priori, it is not obvious how and in what sense the thermal equilibrium can be reached dynamically.

The notion of thermalization in quantum mechanics may be described by the eigenstate thermalization hypothesis (ETH) [1, 2] which gives an understanding of how an observable thermalizes to its thermal equilibrium value. According to ETH for sufficiently complex quantum systems the energy eigenstates are indistinguishable from thermal states with the same average energy.

Although, it is believed that a non-integrable model will generally thermalize, the nature of thermalization might be different in different situations. Actually, besides Hamiltonian which gives dynamics of the system, the nature of the thermalization may also depend on the initial state, such that, within a fixed model different initial states may exhibit different behaviors [3].

To explore this point better let us consider spin- $\frac{1}{2}$

Ising model given by the following Hamiltonian

$$H = -J \sum_{i=1}^{N-1} \sigma_i^z \sigma_{i+1}^z - \sum_{i=1}^N (g\sigma_i^x + h\sigma_i^z). \quad (1)$$

Here and in what follows  $\sigma^{x,y,z}$  are Pauli matrices and  $J, g$  and  $h$  are constants which define the model. By rescaling one may set  $J = 1$ , and the nature of the model, being chaotic or integrable, is controlled by constants  $g$  and  $h$ . In particular, for  $gh \neq 0$  the model is non-integrable. In what follows to perform our numerical computations we will set  $h = 0.5$ ,  $g = -1.05$  [3]. It has been shown in [3] that three different initial states in which all spins are aligned on  $x, y$  or  $z$  directions denoting by  $|X+\rangle, |Y+\rangle, |Z+\rangle$  respectively, results in three distinct thermalization behaviors.

In general, we would like to study time evolution of expectation value of a local operator (observable)  $\mathcal{O}$

$$\langle \psi(t) | \mathcal{O} | \psi(t) \rangle = \text{Tr} (e^{-iHt} \rho_0 e^{iHt} \mathcal{O}), \quad (2)$$

whose behavior could explore the nature of thermalization whether it is strong or weak. In the strong thermalization, the expectation value relaxes to the thermal value very fast, while for weak thermalization it strongly oscillates around the thermal value, though its time average attains the thermal value. Here  $\rho_0$  is density state associated with the initial state  $|\psi_0\rangle$ .

For the Ising model (1) it has been shown that although the initial state  $|Y+\rangle$  exhibits strong thermalization, for initial state  $|Z+\rangle$  one observes weak thermalization and for initial state  $|X+\rangle$  there is an apparent departure of the thermal expectation value from its thermal value suggesting that there might be no thermalization for this state<sup>1</sup> [3].

<sup>1</sup> Actually it seems that the apparent departure of thermalization in this case is due to the finite  $N$  effects and indeed, even in this case we still have a weak thermalization [4].

It was proposed in [3] that whether we are going to observe strong or weak thermalization is closely related to the effective inverse temperature,  $\beta$ , of the initial state which can be read from the following equation

$$\text{Tr}(H(\rho_0 - \rho_{th})) = 0, \quad (3)$$

where  $\rho_{th} = \frac{e^{-\beta H}}{\text{Tr}(e^{-\beta H})}$  is thermal density state with inverse temperature  $\beta$ . The strong thermalization occurs when the effective inverse temperature of initial states is close to zero. On the other hand, for initial states whose effective inverse temperature are sufficiently far away from zero, one observes weak thermalization. In particular, for the model given in (1) the initial state  $|Y+\rangle$  has zero effective inverse temperature and for initial states  $|Z+\rangle$  and  $|X+\rangle$  one has  $\beta = 0.7275$  and  $\beta = -0.7180$ , respectively.

For a given initial state  $|\psi_0\rangle$  the equation (3) may be rewritten as follows

$$\text{Tr}(\rho_{th}H) = \langle \psi_0 | H | \psi_0 \rangle = E, \quad (4)$$

which suggests that the information of the effective inverse temperature could be read from the expectation value of the energy. Indeed, the regime on which the strong or weak thermalization may occur could be also identified by the normalized energy of the initial state [5]

$$\mathcal{E} = \frac{\langle \psi_0 | H | \psi_0 \rangle - E_{min}}{E_{max} - E_{min}} \quad (5)$$

where  $E_{max}, E_{min}$  are maximum and minimum energy eigenvalues of the Hamiltonian. Actually, the quasiparticle explanation of weak thermalization suggests that initial states with weak thermalization are in the regime of near the edge of energy spectrum [6].

Although in the literature, mainly, the normalized energy (5) has been considered to study weak and strong thermalization, it is found useful to work with the expectation value of energy itself which contains the same amount of information as that of the normalized energy.

To further explore the nature of thermalization in the Ising model (1), let us consider an arbitrary initial state in the Bloch sphere which may be parameterized by two angles  $\theta$  and  $\phi$  as follows<sup>2</sup>

$$|\theta, \phi\rangle = \prod_{i=1}^N \left( \cos \frac{\theta}{2} |Z+\rangle_i + e^{i\phi} \sin \frac{\theta}{2} |Z-\rangle_i \right), \quad (6)$$

where  $|Z\pm\rangle$  are eigenvectors of  $\sigma^z$  with eigenvalues  $\pm$ . Indeed, at each site the corresponding state is the eigenvector of the operator  $\mathcal{O}_i = n \cdot \sigma_i$ , with  $n$  is the unit vector on the Bloch sphere. More explicitly, one has

$$\mathcal{O}_i(\theta, \phi) = n \cdot \sigma_i = \cos \theta \sigma_i^z + \sin \theta (\cos \phi \sigma_i^x + \sin \phi \sigma_i^y), \quad (7)$$

for  $i = 1, \dots, N$ .

For this general initial state and for the model (1) one can compute the expectation value of energy which has the following simple form

$$E = -\cos \theta (Nh + (N-1)J \cos \theta) - Ng \cos \phi \sin \theta. \quad (8)$$

An interesting feature of the expectation value of energy is that for large  $N$  ( $N \gg 1$ ), the number of spins appears as an overall factor and thus the density of energy defined by  $E/N$  (energy per site) is independent of the size of the system

$$\frac{E}{N} \approx -(h \cos \theta + J \cos^2 \theta) - g \cos \phi \sin \theta, \quad N \gg 1. \quad (9)$$

Using this analytic expression for the expectation value of energy we have drawn the density of energy in figure 1 for  $N = 100$  and  $J = 1, h = 0.5, g = -1.05$ . Actually, to highlight the regions where the density of energy vanishes we have depicted its absolute value.

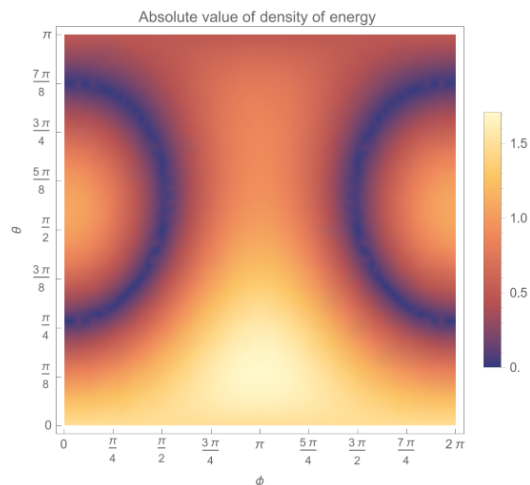


Figure 1. Absolute value of the density of energy evaluated using the analytic expression (8) for  $N = 100$  and  $J = 1, h = 0.5, g = -1.05$ .

To compare this result with the behavior of the effective inverse temperature and in particular the sensitivity of the result with the size of the system, in figure 2 we have presented the numerical result of the absolute value of the effective inverse temperature for  $N = 7$ . Since the Hamiltonian of the model (1) is traceless, the locus of  $\beta = 0$  are given by the regions over which  $E = 0$  that are shown by two dark semi circles (ring of zero  $\beta^3$ ) in figures 1 and 2. This is, particularly, illustrative since the main significant information contained in  $\beta$  is its distance

<sup>2</sup> In general the initial state could be identified by  $2N$  angles  $(\theta_i, \phi_i)$  for  $i = 1, \dots, N$ . In our case we have assumed that angles in all sites are equal.

<sup>3</sup> By a phase shift one may draw the density of energy for  $-\pi \leq \phi \leq \pi$  for which  $\beta = 0$  region is a ring.

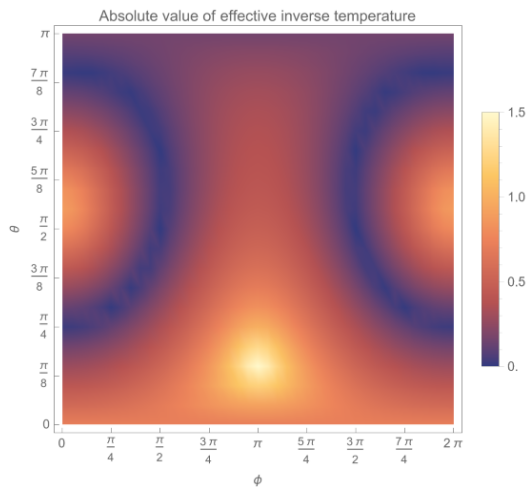


Figure 2. Absolute value of the effective inverse temperature for arbitrary  $\theta, \phi$  for the general initial state (6). Here we have set  $N = 7$  and  $g = 0.5$ ,  $h = -1.05$ .

(absolute value) from zero. Generally, it is believed that strong thermalization occurs near the ring of zero  $\beta$ .

One observes that the behavior of the effective inverse temperature matches exactly that of the density of energy event though the size of the two systems by which these quantities are evaluated are different by about a factor of 15. This shows the robustness of the results against the size of the system. In particular, this has to be compared with the results in the literature where the numerical computations have been performed for  $N = 14$ . Even though our  $\beta$  is evaluated for  $N = 7$  in comparison with that of  $N = 14$  the error we acquire is about 3 percent.

The aim of the present article, which will be explored in the next section, is to study quantum thermalization using the Krylov basis which seems more appropriate basis when the dynamics of the system is of our interest. Within this context, we will also study the nature of thermalization.

## II. KRYLOV BASIS AND THERMALIZATION

Let us consider a closed quantum system with time independent local Hamiltonian  $H$  whose eigenstates and eigenvalues are denoted by  $|E_n\rangle$ , and  $E_n$ , respectively. Starting with an initial state,  $|\psi_0\rangle$ , in the Schrödinger picture at any time one has

$$|\psi(t)\rangle = e^{iHt}|\psi_0\rangle. \quad (10)$$

In the context of quantum thermalization the main purpose is to start with an initial state and then quickly alter the system, *e.g.* by a global quench, and then let the system evolve under the local Hamiltonian  $H$ . As we have already mentioned, generally, we are interested in

the late time behavior of the expectation value of local operators (observables)

$$\langle\psi(t)|\mathcal{O}|\psi(t)\rangle = \langle\psi_0|e^{-iHt}\mathcal{O}e^{iHt}|\psi_0\rangle = \langle\mathcal{O}(t)\rangle. \quad (11)$$

The main question is to what extent and for what times the system can be described by a suitable thermal equilibrium system in which the above expectation value can be approximated by  $\text{Tr}(\rho_{th}\mathcal{O})$ .

To study different features of chaotic systems and thermalization one usually utilizes the energy spectrum and energy eigenstates which amounts to diagonalize the Hamiltonian. For example, the nature of quantum chaos may be given in terms of the energy level statistics [7].

In the energy eigenstates the expectation value (11) reads

$$\langle\mathcal{O}(t)\rangle = \overline{\langle\mathcal{O}\rangle} + \sum_{n \neq m}^{\mathcal{D}} e^{i(E_n - E_m)t} c_n c_m^* \langle E_m | \mathcal{O} | E_n \rangle \quad (12)$$

where  $\mathcal{D}$  is the dimension of Hilbert space,  $c_n$  is coefficient of expansion of the initial state in energy basis and  $\overline{\langle\mathcal{O}\rangle}$  stands for infinite time average:  $\overline{\langle\mathcal{O}\rangle} = \frac{1}{T} \int_0^T \langle\mathcal{O}(t)\rangle dt$  for  $T \rightarrow \infty$  limit. Then, one can proceed to explore equilibrium and thermalization in this context which happens due to the possible phase cancellation in long times [8].

We note, however, that a Hamiltonian may be also put into a tridiagonal form in which we could work in the Krylov basis. See *e.g.* [9–11]. In this basis, we usually deal with Lanczos coefficients and thus we would expect that the properties of the quantum system can be also described in terms of the spectrum of Lanczos coefficients. Indeed, the Lanczos spectrum has been used to study operator growth in many body systems [12] (see also [13]). Recently, it was also suggested in [11] that the chaotic nature of a system may be described in terms of the Lanczos coefficients. More precisely, it was proposed that “Quantum chaotic systems display a Lanczos spectrum well described by random matrix model.”

### A. Thermalization in Krylov basis

Here we would like to study quantum thermalization in the Krylov basis. In particular, we would like to understand to what extent the nature of thermalization may be explored in this context. To proceed, let us first briefly review the recursive procedure producing the Krylov space for a given state in a quantum system (see [14] for review).

Starting with an initial state  $|\psi_0\rangle$  in a quantum system with a time independent Hamiltonian  $H$ , the Krylov basis,  $\{|n\rangle, n = 0, 1, 2, \dots, \mathcal{D}_\psi - 1\}$ , can be constructed as follows. The first element of the basis is identified with the initial state  $|0\rangle = |\psi_0\rangle$  (which we assume to be normalized) and then the other elements are constructed, recursively, as follows

$$|\widehat{n+1}\rangle = (H - a_n)|n\rangle - b_n|n-1\rangle, \quad (13)$$

where  $|n\rangle = b_n^{-1}|\hat{n}\rangle$ , and

$$a_n = \langle n|H|n\rangle, \quad b_n = \sqrt{\langle \hat{n}|\hat{n}\rangle}. \quad (14)$$

This recursive procedure stops whenever  $b_n$  vanishes which occurs for  $n = \mathcal{D}_\psi \leq \mathcal{D}$  that is the dimension of Krylov space. Recall that  $\mathcal{D}$  is the dimension of the Hilbert space of the quantum system. Note that this procedure produces an orthonormal and ordered basis together with coefficients  $a_n$  and  $b_n$  known as the Lanczos coefficients [15].

Having constructed the Krylov basis, at any time the evolved state may be expanded in this basis

$$|\psi(t)\rangle = \sum_{n=0}^{\mathcal{D}_\psi-1} \phi_n(t) |n\rangle, \quad \text{with} \quad \sum_{n=0}^{\mathcal{D}_\psi-1} |\phi_n(t)|^2 = 1, \quad (15)$$

where the wave function  $\phi_n(t)$  satisfies the following Schrödinger equation

$$-i\partial_t \phi_n(t) = a_n \phi_n(t) + b_n \phi_{n-1}(t) + b_{n+1} \phi_{n+1}(t), \quad (16)$$

which should be solved with the initial condition  $\phi_n(0) = \delta_{n0}$ .

In this formalism the expectation value of a local operator (11) reads

$$\begin{aligned} \langle \mathcal{O}(t) \rangle &= \sum_{n,m=0}^{\mathcal{D}_\psi-1} \phi_n^*(t) \phi_m(t) O_{nm} \\ &= \sum_{n=0}^{\mathcal{D}_\psi-1} |\phi_n(t)|^2 O_{nn} + \sum_{n \neq m=0}^{\mathcal{D}_\psi-1} \phi_n^*(t) \phi_m(t) O_{nm} \end{aligned} \quad (17)$$

where  $O_{nm} = \langle n|\mathcal{O}|m\rangle$  are matrix elements of the operator  $\mathcal{O}$  in the Krylov basis which, in general, are complex numbers. Of course, the diagonal elements are real.

The infinite time average of the corresponding operator is given by

$$\overline{\langle \mathcal{O} \rangle} = \sum_{m,n=0}^{\mathcal{D}_\psi-1} C_{nm} O_{nm}, \quad (18)$$

where

$$C_{nm} = \lim_{T \rightarrow \infty} \int_0^T dt \phi_n^*(t) \phi_m(t), \quad (19)$$

is a complex matrix with the conditions  $C_{nm}^* = C_{mn}$  and  $\sum_n C_{nn} = 1$ . Following the idea of ETH, in our framework, in order to get an infinite time average consistent with the macro canonical result, one may assume that the matrix elements,  $O_{nm}$ , should satisfy an ETH like condition

$$O_{nm} \sim O \delta_{mn} + \mathcal{O}(\mathcal{D}^{-1}), \quad (20)$$

by which we are guaranteed to get the expected thermal equilibrium for the expectation value of the corresponding operator. Here  $O$  is a constant. One may want to call

this remarkable behavior as Krylov basis thermalization hypothesis (KTH).

To examine KTH behavior of local operators (observables) we will compute the matrix elements of the operator  $S_x = \sum_{i=1}^N \sigma_i^x$ , which is magnetization in the  $x$  direction, for the Ising model (1) with  $h = 0.5$ ,  $g = -1.05$  where the model is non-integrable.

The corresponding matrix elements for two different initial states  $|Y+\rangle$  and  $|Z+\rangle$  are presented in figure 3 for  $N = 10$ . From this figure, one observes that the matrix elements  $O_{nm}$  exhibit desired behavior as imposed by KTH indicating that thermalization occurs for both cases, as expected.

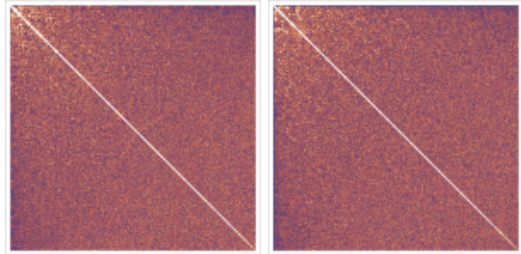


Figure 3. Matrix elements of the operator  $S_x = \sum_i \sigma_i^x$  in Krylov basis for cases where the initial state is  $|Y+\rangle$  (left) and  $|Z+\rangle$  (right). Darker points represent the matrix elements that are closed to zero.

To highlight the behavior of matrix elements we have presented the absolute value of them, so that in figure 3 the dark points correspond to vanishing elements. Note that, in general, the off diagonal matrix elements are complex numbers and what has been depicted in this figure is the real part of the matrix elements.

In comparison with ETH where matrix elements of operators in energy eigenstates are real, having complex off diagonal elements in KTH makes the situation more involved. Indeed, one should also examine the imaginary part of the off diagonal matrix elements that contribute to off diagonal terms in the expectation value of the operators. It also requires to study of the behavior of  $C_{nm}$  as well.

We have also computed matrix elements of the magnetization in the  $z$  direction,  $S_z = \sum_{i=1}^N \sigma_i^z$ , for several initial states specified by different  $\theta$  and  $\phi$  and we have found the same pattern as that in figure 3. Although in all cases we have considered, our numerical computations support the KTH proposal, we think it is interesting to explore this point better [16].

To further explore the KTH behavior we have also done the same computations for the cases where  $gh = 0$  in which the model (1) is integrable. An immediate observation we have made is that in integrable cases the dimension of Krylov space reduces significantly<sup>4</sup> which may

<sup>4</sup> Similar observation has been already made in the context of op-

also depend on the initial state. For example, for  $N = 10$  while in the chaotic case the dimension of Krylov space is 529, in an integrable mode given by  $h = 0$ ,  $g = -1.05$  it is 463 for initial states  $|Y+\rangle$ ,  $|Z+\rangle$  and 253 for  $|X+\rangle$ . For integrable model given by  $h = 0.5$ ,  $g = 0$  it is 23 for  $|Y+\rangle$ ,  $|X+\rangle$  and zero for  $|Z+\rangle$ .

In order to have a better statistic we have considered the case where  $h = 0$ ,  $g = -1.05$ . For this case, we have computed matrix elements of different operators in the Krylov basis for different initial states. We have found that, although for some special cases the corresponding matrix elements have almost similar pattern as that in figure 3, it is not a generic behavior and typically they exhibit non-universal behavior. Actually, even in some cases the real part of the matrix elements are identically zero.

It is worth noting that there is a special operator in Krylov space whose matrix elements is exactly diagonal. More precisely, consider the number operator defined by

$$\mathcal{N} = \sum_{n=0}^{\mathcal{D}_\psi-1} n|n\rangle\langle n|, \quad (21)$$

that is obviously diagonal in Krylov basis,  $\mathcal{N}_{nm} = n\delta_{nm}$ . In this case the expectation value (11), actually, computes Krylov complexity [12]

$$\mathcal{C} = \langle \mathcal{N}(t) \rangle = \sum_{n=0}^{\mathcal{D}_\psi-1} n |\phi_n(t)|^2, \quad (22)$$

that saturates (equilibrate) at very late times where the Lanczos coefficients vanish [19].

## B. Krylov space and nature of thermalization

Restricting ourselves to the non-integrable phase, as it is clear from the above construction, the Lanczos coefficients should contain information about both the dynamics of the model and the initial state making it a suitable candidate to probe the nature of thermalization. Therefore, it is natural to see if they could also probe weak and strong thermalization. In particular, although both initial states  $|Y+\rangle$  and  $|Z+\rangle$  exhibit almost the same pattern for the operator matrix elements, indicating that both states yield to thermalization, we are wondering if it is possible to distinguish between the nature of thermalization for these states using the properties of Lanczos coefficients.

To proceed, let us first compute Lanczos coefficients for three distinct initial states we have considered in the previous section<sup>5</sup>. The results for  $N = 10$  are shown in figure 4

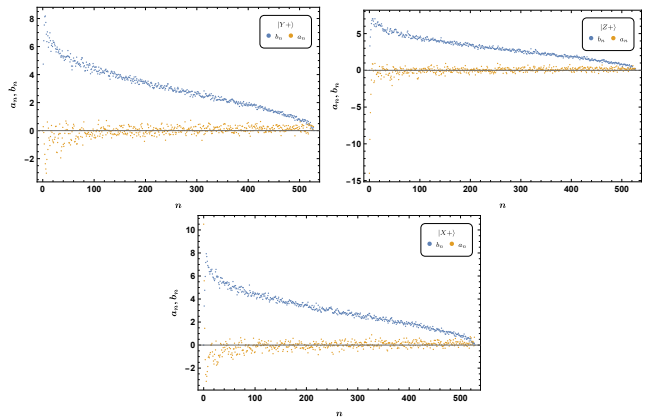


Figure 4. Lanczos coefficients  $a_n, b_n$  of three initial states  $|Y+\rangle, |Z+\rangle, |X+\rangle$ .  $b_n$  and  $a_n$  are shown with blue and brown circles, respectively. The numerical results are presented for  $N = 10$  in which the dimension of Krylov space for a generic initial state is about 529.

Although one could recognize some differences between these three plots, the differences are not significant and essentially the Lanczos coefficients for all three cases have qualitatively the same behavior. Therefore, one may want to conclude that the naive behavior of Lanczos coefficients could not provide a quantity to make a distinction between these three cases.

We note, however, that a better quantity which might be more sensitive to the initial state is the variance of Lanczos coefficients. Indeed, the variance of Lanczos coefficients has been considered in [23] as a measure to probe whether a system is chaotic or integrable.

Let us recall that for a collection of  $M$  numbers,  $s_i$ , the variance may be defined as follows

$$\text{Var}(s_i) = \frac{1}{M} \sum_{i=1}^M (s_i - \bar{s})^2 \quad (23)$$

where  $\bar{s}$  is the mean value. In what follows we would like to compute the variance of Lanczos coefficients  $a_n$  and  $b_n$ . Actually, if one computes the variance of Lanczos coefficients for three initial states considered before, one observes that they differ significantly.

More generally, one could compute the variance of Lanczos coefficients associated with the general initial state given by (6). In figure 5 we have presented the numerical results for the variance of  $a_n$  and  $b_n$  as a function of  $\theta$  and  $\phi$  for  $N = 10$ .

Clearly, there is an obvious correlation between behaviors of the effective inverse temperature, the absolute value of the density of energy (or normalized energy) and variance of Lanczos coefficients (see figure 1). Generally, one observes that for regions where the effective inverse temperature is small the variance of  $a_n$  ( $b_n$ ) is also small (large). The variance of  $a_n$  ( $b_n$ ) becomes larger (smaller) as we move away from  $\beta = 0$  regions. Another observation we have made is that being positive, the variance is

erator Krylov complexity in [17] (see also [18]).

<sup>5</sup> Lanczos coefficients for the model under consideration have also been computed in [20–23].

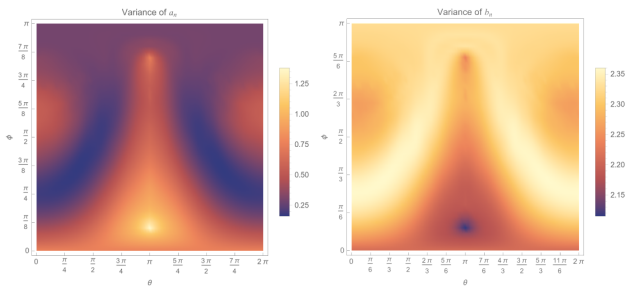


Figure 5. Variance of Lanczos coefficients  $a_n$  (left) and  $b_n$  (right). The numerical results are done for  $N = 10$  spins.

not sensitive to the sign of  $\beta$  and only the absolute value of it matters.

We note, however, that the behavior of variances is not exactly the same as that of effective inverse temperature. Indeed, even though one can recognize the lower part of the ring of zero  $\beta$ , the upper part is not apparent in the plots of variances, though there is a trace of the ring. More precisely, although from the behavior of  $\beta$  or density of energy one would expect to see states with strong thermalization are localized near the ring of zero  $\beta$ , the behavior of the variance suggests that strong thermalization for states with  $\theta \gtrsim \frac{2\pi}{3}$  does not necessarily located near the ring of zero  $\beta$  and rather they almost uniformly distribute around  $\theta \approx \pi$ .

As a final observation, one notices that at the symmetric axis of  $\phi = \pi$ , while the effective inverse temperature or the absolute value of the density of energy decreases almost monotonically from  $\theta = \frac{\pi}{6}$  to  $\theta = \pi$ , the variance of  $a_n$  exhibits a pick around  $\theta \approx \frac{5\pi}{6}$  suggesting that the state  $|\frac{5\pi}{6}, \pi\rangle$  would be among those with the weakest thermalization.

Actually, since we have an exact analytic expression for the energy one can use it as a gauge to validate our numerical results. In fact, by making use of the analytic expression of energy we can compute the density of energy for  $\phi = \pi$  slice for arbitrary  $N$ . In figure 6 we have drawn the density of energy for  $\phi = \pi$  slice for  $N = 10$  and 100. We have also presented the first derivative of the density of energy to better explore its behavior.

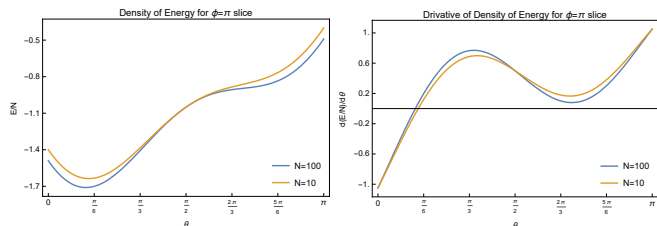


Figure 6. Density of energy (left) and its derivative (right) for  $\phi = \pi$  slice for different  $N = 10, 100$ . Indeed, they show nontrivial behavior around  $\theta = \frac{5\pi}{6}$ , though it is not as pronounced as that in the variance of  $a_n$ .

From this figure, one finds that the density of energy, indeed, exhibits a non-trivial behavior around  $\theta = \frac{5\pi}{6}$ , though it is not as pronounced as that in the variance of  $a_n$ . Actually, the first derivative is closed but not exactly zero showing that there is no real minimum around the position of the second pick, even though for higher  $N$  the situation gets better. Therefore, although the general behavior of the variance of Lanczos coefficients are consistent with the results of other probes, we have seen slightly mismatch at  $\phi = \pi$  slice.

Working with Krylov basis, yet another interesting quantity one may consider as a possible measure to probe the nature of thermalization is Krylov complexity (22). Indeed, by making use of the fact that the Krylov complexity is essentially the expectation value of the number operator, one can compute the infinite time average of Krylov complexity [24] and consider it as a possible probe. More precisely, from the expression of Krylov complexity (22) one has

$$\bar{C} = \lim_{T \rightarrow \infty} \frac{1}{T} \int_0^T \langle \mathcal{N}(t) \rangle dt = \sum_{n=0}^{\mathcal{D}_\psi - 1} n C_{nn}. \quad (24)$$

It is then straightforward to compute the infinite time average of complexity for states associated with initial states (6). The numerical result for  $N = 9$  is depicted in figure 7.

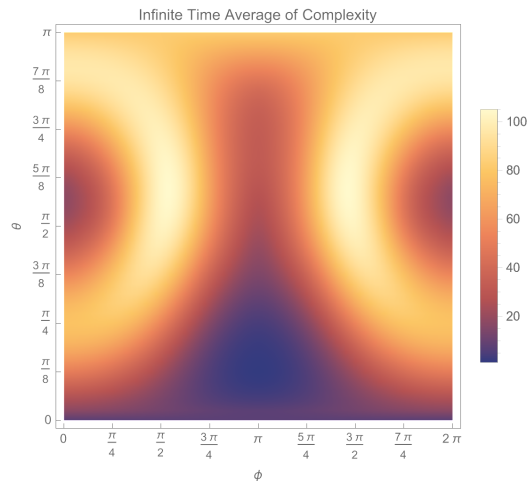


Figure 7. Infinite time average of complexity for states associated with the initial state 6. The numerical computation is done for  $N = 9$ .

Interestingly enough, the resultant pattern is exactly compatible with those of the absolute value of the density of energy and the effective inverse temperature. In particular, we have found that for states exhibiting strong thermalization the saturation value for complexity is larger.

To get a better understanding of what exactly happens in different points in  $\theta - \phi$  plane (initial states), it is useful to explicitly compute the expectation value of local operators to see how the thermalization occurs for

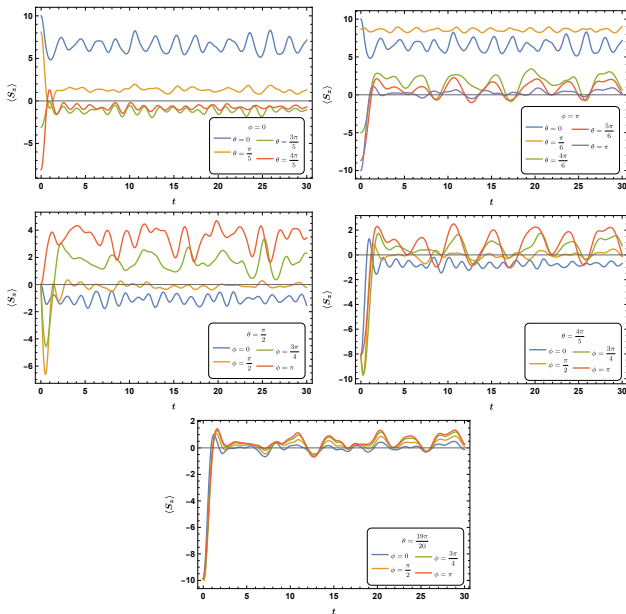


Figure 8. Expectation value of  $S_z$  as a function of time for different initial states. As we see the weakest thermalization mostly occurs for states whose theta angle is near zero while beside the ring of zero  $\beta$  the strong thermalization occurs for  $\theta \approx \pi$ .

different initial states. To do so, we will consider the magnetization in the  $z$  direction and compute the following quantity <sup>6</sup>

$$\langle S_z(t) \rangle = \langle \theta, \phi | e^{-iHt} \sum_{i=1}^N \sigma_i^z e^{iHt} | \theta, \phi \rangle, \quad (25)$$

for different values of  $\theta$  and  $\phi$ . The results are depicted in figure 8. Actually, we have computed the corresponding expectation value for 441 initial states<sup>7</sup> and only few of them have been shown in this figure which are for particular slices given by  $\phi = 0, \pi$  and  $\theta = \frac{\pi}{2}, \frac{4\pi}{5}, \frac{19\pi}{20}$ . The results are relatively compatible with what suggested by the variance of Lanczos coefficients and in exact agreement with what suggested by the infinite time average of complexity.

From the behavior of the expectation value of  $S_z$  one observes that states with weak thermalization are mostly located around  $\theta \approx 0$  while those of strong thermalization are around  $\theta \approx \pi$ , besides those located near ring of zero  $\beta$ . Thus, as one moves from  $\theta = 0$  towards  $\theta = \pi$ , generally, states show stronger thermalization. Interestingly

enough, one finds that the initial states  $|Y+\rangle, |Z+\rangle$  and  $|X+\rangle$  are not among those states with the strongest or weakest thermalization. It is in contrast with the general belief that states with strong thermalization are located near the ring of zero  $\beta$ . In particular, states  $|Z+\rangle = |0, \phi\rangle$  and  $|Z-\rangle = |\pi, \phi\rangle$ , for arbitrary  $\phi$ , exhibit weak and strong thermalization, respectively.

To be more concrete let us look at  $\phi = 0$  slice where we have presented results for  $\theta = 0, \frac{\pi}{5}, \frac{\pi}{2}, \frac{3\pi}{5}, \frac{4\pi}{5}, \frac{19\pi}{20}, \pi$  in figure 8. By making use of these results one finds that at  $\theta = 0$  we have weak thermalization though it becomes stronger as one approaches the ring of zero  $\beta$ . Then it becomes weaker as one moves further forwards  $\frac{\pi}{2}$  after which it keeps becoming stronger all the way to  $\theta = \pi$ . Interestingly enough, we have found that the behavior is consistent with the behavior of the infinite time average of complexity which is also in qualitative agreement with the behavior of the variance of Lanczos coefficients.

For  $\theta = \frac{\pi}{2}$  slice, one finds very weak thermalization at  $\phi = 0$  and then it becomes very strong at  $\theta = \frac{\pi}{2}$  where the slice intersects the ring of zero  $\beta$ . Then, it becomes weaker as one moves towards  $\theta = \pi$  point. For  $\theta = \frac{4\pi}{5}$  slice, we get strong thermalization almost on the whole slice, though it shows slightly stronger behavior in a point where the slice intersects the region of zero  $\beta$ . Of course, they become relatively weaker as one moves towards  $\phi = \pi$ . Finally, for  $\theta = \frac{19\pi}{20}$  slice one has always strong thermalization all the way from  $\phi = 0$  to  $\phi = \pi$ .

An interesting observation we have made is that, unlike the  $\theta = \frac{\pi}{2}, \frac{4\pi}{5}$  slices where we see a significant change at the ring of zero  $\beta$ , for  $\theta = \frac{19\pi}{20}$  slice the change is not so significant, in agreement with the behavior of the variance and the infinite time average of complexity.

Looking at  $\phi = \pi$  slice, from the expectation value of  $S_z$  we find that the weakest thermalization occurs at  $\theta \approx \frac{\pi}{6}$  while it becomes relatively stronger as we move towards  $\theta = \pi$ . Surprisingly, we did not observe any further special point in this slice in agreement with the behavior of the infinite time average of complexity and in contrast to the behavior suggested by the variance in which we would expect to have a state with relatively weaker thermalization around  $\theta \approx \frac{5\pi}{6}$ .

### C. Inverse participation ratio

It is worth mentioning that the nature of weak and strong thermalization for certain XY Ising model has been studied in [25] by making use of the inverse participation ratio [26]. Thus it is worth looking at this quantity for our model too.

Consider a state whose expansion in the energy eigenstates is  $|\psi\rangle = \sum_{i=1}^{\mathcal{D}} c_i |E_i\rangle$ , where  $c_i = \langle E_i | \psi \rangle$ . Then, the inverse participation ratio is defined by

$$\lambda = \frac{1}{\sum_{i=1}^{\mathcal{D}} |c_i|^4}, \quad (26)$$

<sup>6</sup> We have also computed the expectation value for the magnetization in the  $x$  direction,  $S_x$ , in which we have found that the conclusion is the same as that of  $S_z$  that is explicitly presented in what follows.

<sup>7</sup> Since the pattern in the figure 5 is symmetric under  $\phi \rightarrow 2\pi - \phi$ , we have only considered initial states located in  $0 \leq \phi \leq \pi$ .

that is essentially a quantity that measures the number of energy eigenstates that contribute to the state  $|\psi\rangle$ . Note that  $1 \leq \lambda \leq \mathcal{D}$ . In fact, when only one energy eigenstate contributes to the state the inverse participation number is one, while when all energy levels equally contribute to the state it is equal to  $\mathcal{D}$ .

Now let us compute the inverse participation ratio for general initial state (6). The result is depicted in figure 9. Note that what is drawn in this figure is the logarithm of the inverse participation ratio,  $\ln \lambda$ . Interestingly enough, one observes a significant correlation with all quantities we have considered so far, including the variance of Lanczos coefficients.

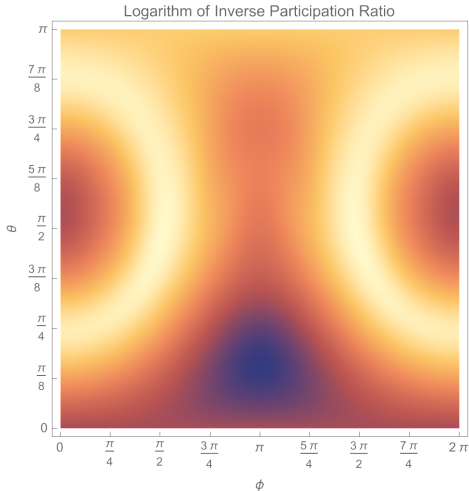


Figure 9. The logarithm of inverse participation ratio for general initial state given in (6) as a function of  $\theta$  and  $\phi$ . The numerical computation is done for  $N = 10$ .

It is worth noting that the behavior of the inverse participation ratio is in perfect agreement with that of the infinite time average of complexity. It shows that the saturation value for complexity is greater for states consisting of more energy eigenstates [23, 24].

It is important to note that using the behavior of the effective inverse temperature and normalized energy it was suggested that the weak thermalization occurs for the states for which the expectation value of the energy is near the edge of the energy spectrum [3–6]. Here, we have seen that whether a state exhibits weak or strong thermalization is correlated to its inverse participation ratio as suggested in [25]. More precisely, the nature of the thermalization of a state is closely related to the number of energy eigenstates that contribute to the state. A state consisting of more energy eigenstates likely exhibits stronger thermalization. Note that our computations of the expectation value of local operators confirm this behavior too.

It is also interesting to see that looking at  $\phi = \pi$  slice, we get similar behavior as that in the variance of Lanczos coefficients, namely, there are two picks around  $\frac{\pi}{6}$  and

$\frac{5\pi}{6}$ . Unlike the variance of Lanczos coefficients in this case one can see that although the first pick represents the state with the weakest thermalization, the second pick is the artifact of the finite  $N$  effect. To see this, we have presented the logarithm of the inverse participation ratio for  $N = 10$  and  $N = 11$  in figure 10 from which it is evident that the second pick is removed as we go to higher  $N$ . Interestingly enough, the correction due to higher  $N$  does not significantly alter other features of the inverse participation ratio.

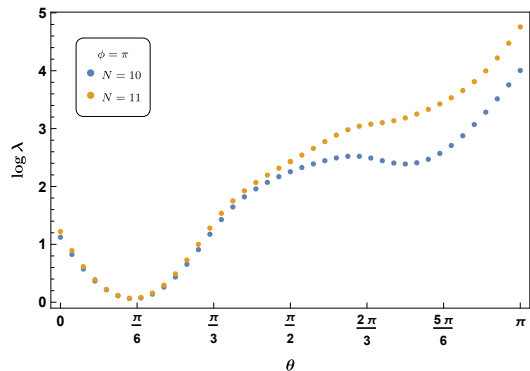


Figure 10. The logarithm of inverse participation ratio of  $\phi = \pi$  slice for  $N = 10, 11$ . One observes that the second pick (minimum) is removed as one goes to higher  $N$ .

It is also interesting that for  $N = 11$  the behavior of inverse participation ratio at  $\phi = \pi$  is very close to that of the density of energy (see figure 6).

### III. DISCUSSIONS

In this paper, we have studied thermalization for a closed quantum system using the Krylov basis. Actually, our main motivation to do so is that, by definition, under time evolution a quantum state propagates over a subspace of Hilbert space known as Krylov space. An advantage (at least theoretically) of working in this space is that we will have to deal with a space whose dimension is usually smaller than the dimension of the Hilbert space.

In the traditional approach to quantum thermalization one usually has to study the expectation value of operators in the energy eigenstates. It is believed that for a chaotic quantum system the thermalization occurs in the level of eigenstates that mathematically reflected in the statement of ETH.

On the other hand, working within the context of Krylov space, one will have to compute matrix elements of local operators in the Krylov basis. It is then natural to expect that a similar concept may also show up in this context. Indeed, by making use of an explicit example we have shown that the matrix elements of local operators satisfy a similar condition as that in ETH.

We note, however, that unlike in the energy eigenstates



matrix elements in Krylov basis are generally complex numbers. Therefore, in this case the situation is more complicated than ETH. Indeed, what we have shown is that the real part of the matrix elements follows a similar behavior as that of ETH and thus we called the statement as Krylov basis thermalization hypothesis (KTH).

For a given operator the contribution of the imaginary part is in the off diagonal terms that may cause an oscillatory behavior over thermal equilibrium value which could affect the natural of the thermalization. It is interesting to understand this point better[16].

We note that the nature of thermalization depends on two important ingredients: the Hamiltonian of the system and the initial state. As we have seen, by construction, the Krylov basis and Lanczos coefficients contain information about these ingredients making them nature objects to probe the nature of thermalization.

We have shown that the infinite time average of Krylov complexity could provide a measure to probe the nature of thermalization. We have seen that the behavior of the infinite time average of complexity is in perfect agreement with the behaviors of the effective inverse temperature and the density of energy. In particular, an initial state exhibiting strong thermalization has relatively larger value for complexity saturation.

We have also suggested that the variance of Lanczos coefficients could probe the nature of thermalization to see whether for a given initial state the thermalization is weak or strong, too. We have seen that a state with relatively smaller (greater) variance for Lanczos coefficients  $a_n$  ( $b_n$ ) exhibits strong (weak) thermalization. Of course, there is some mismatch between the variance of Lanczos coefficients and the other quantities we have evaluated. We believe that this miss match might be due to the finite  $N$  effect, though to explicitly show it we need to go to sufficiently higher  $N$  and perform our numerical computations with extremely high precision which is out of our computational abilities. We leave exploring this point for further study.

To further explore the thermalization properties of the model under consideration we have also evaluated the inverse participation ratio for general initial states. We have observed that strong thermalization occurs for states with relatively greater inverse participation ratio. In other words, a state consisting of more energy eigenstates is more likely to exhibit stronger thermalization. We have seen that there is a direct relation between the behaviors of the infinite time average of complexity and the inverse participation ratio.

To verify our proposal we have also computed the time dependence of the expectation value of local operators to explicitly probe the nature of thermalization for the generic initial state given by (6). The results, indeed, confirm our observation based on the behaviors of the infinite time average complexity, the inverse participation ratio and the variance of Lanczos coefficients.

An interesting question we have been trying to address rather implicitly in this paper was the robustness of the

quantities we have studied in this paper against the size of the system. In most numerical computations we have done in this paper we have set  $N = 10$ , while in the literature the computations are done for  $N = 14$ . It is then natural to see how robust the results are.

Actually, among all the quantities we have considered in this paper, we have presented an exact analytic expression for expectation value of energy which may be treated as a gauge to validate other results.

It is clear from the exact analytic expression that for large  $N$  limit the density of energy is independent of  $N$ , so that its behavior is universal which only depends on the parameters of the model  $g$  and  $h$ .

We have also computed effective inverse temperature for  $N = 7$  and, surprisingly, one observes that it perfectly agrees with the density of energy even for large  $N$ , showing that the behavior of  $\beta$  is robust against the size of the system. Of course, as we have already mentioned the actual value of  $\beta$  is changed, though in comparison with the numerical results available in the litterateur for  $N = 14$  one finds just a few percent errors. It is worth emphasizing that this is also the case for other quantities we have studied in this paper that include the infinite time average of complexity, the inverse participation number and the expectation value of local operators. We note, however, that for the variance of Lanczos coefficients, we expect to see significant finite  $N$  effect to make it consistent with other quantities.

To explore our idea about thermalization in the Krylov basis we have considered an Ising model whose Hamiltonian is given by (1). We note, however, that there is another model which has been extensively studied in the literature whose Hamiltonian is

$$H = \sum_{i=1}^{N-1} \sigma_i^x \sigma_{i+1}^x + \sigma_i^y \sigma_{i+1}^y + g \sum_{i=1}^N \sigma_i^y. \quad (27)$$

For the general initial state (6) the expectation value of the energy is

$$E = \sin \theta ((N - 1) \sin \theta + Ng \sin \phi). \quad (28)$$

One may also explore thermalization and its nature for this model by evaluating different quantities such as the effective inverse temperature and the infinite time average of complexity. Doing so, one can see that the results are consistent with the behavior of the expectation of the energy (28), that also confirms our expectations. We note that the inverse participation ratio for this model has been studied in [25].

In this paper, we have studied the infinite time average of the Krylov complexity and the variance of Lanczos coefficients associated with the spread of an initial state [27]. We note, however, that the same question as studied in this paper can be also addressed using Lanczos coefficients associated with operator growth [12]<sup>8</sup>. Es-

<sup>8</sup> We note that operator and state growth may be studied within a universal framework[28]

essentially in our context, it corresponds to changing the picture from Schrödinger to Heisenberg.

In the Heisenberg picture of quantum mechanics, we are dealing with the operators and the time evolution is attributed to the operator

$$\mathcal{O}(t) = e^{-iHt} \mathcal{O} e^{iHt}. \quad (29)$$

Defining an inner product in the space of operators acting on the Hilbert space, one can construct Krylov basis for the operator starting with an initial operator  $\mathcal{O}$ . The first element is identified with the initial operator  $O_0 = \mathcal{O}$  (which we assume to be normalized with respect to the inner product) and the other elements may be constructed recursively as follows

$$\hat{O}_{n+1} = \mathcal{L}O_n - \hat{b}_n O_{n-1}, \quad O_n = \hat{b}_n^{-1} \hat{O}_n, \quad (30)$$

where  $\mathcal{L}O_n = [H, O_n]$  and  $\hat{b}_n^2 = |\hat{O}_n \cdot \hat{O}_n|$  is Lanczos coefficients. The procedure stops for  $n = \mathcal{D}_O \leq \mathcal{D}^2 - \mathcal{D} + 1$  [17] that is the dimension of Krylov space for the operator. Here we denote the Lanczos coefficients with a hat to avoid confusion with those defined in the Krylov basis for state in (14). Using this basis one has

$$\mathcal{O} = \sum_{n=1}^{\mathcal{D}_O-1} i^n \varphi_n(t) O_n. \quad (31)$$

Note that with this notation  $\varphi_n(t)$  is real and satisfies the following equation

$$\partial_t \varphi_n(t) = \hat{b}_n \varphi_{n-1} - \hat{b}_{n+1} \varphi_{n+1}. \quad (32)$$

In this context, we could also look for the variance of Lanczos coefficients in the operator picture. To study Lanczos coefficients for the Ising model (1) we may consider a generic initial operator as follows

$$\mathcal{O}_{\theta, \phi} = \prod_{i=1}^N \mathcal{O}_i(\theta, \phi), \quad (33)$$

where  $\mathcal{O}_i$  is defined in (7). It is worth noting that since this initial state (6) is the eigenstate of the above operator, in this case we are essentially studying the time evolution of density matrix associated with the initial state  $\mathcal{O}_{\theta, \phi} = \rho(\theta, \phi) = |\theta, \phi\rangle\langle\theta, \phi|$ .

One can also study the variance of Lanczos coefficients  $\hat{b}_n$  associated with the initial density matrix. Doing so, one finds the corresponding variance results in the same conclusion as that for the state studied in the previous section. An interesting observation we have made is that the behavior of variance  $\hat{b}_n$  in operator growth is actually identical with that obtained from  $a_n$  in state growth. It would be interesting to understand this point better[16].

## ACKNOWLEDGEMENTS

We would like to thank Ali Mollabashi, Mohammad Reza Mohammadi Mozaffar, Mohammad Reza Tanhayi and Hamed Zolfi for useful discussions. We would also like to thank the School of Physics of the Institute for Research in Fundamental Sciences (IPM) for providing computational facilities. M.A. Would also like to thank Souvik Banerjee for discussions on different aspects of Krylov space. Some numerical computations related to this work were carried out at IPM Turin Cloud Services [29]. This work is based upon research funded by Iran National Science Foundation (INSF) under project No 4023620.

- 
- [1] M. Srednicki, “Chaos and Quantum Thermalization,” *Phys. Rev. E* **50**, 888 doi:10.1103/PhysRevE.50.888 [arXiv:cond-mat/9403051 [cond-mat]].
- [2] Deutsch JM. Quantum statistical mechanics in a closed system. *Phys Rev A*. **43** (1991) 2046 doi:10.1103/physreva.43.2046
- [3] M. C. Bañuls, J. I. Cirac and M. B. Hastings, “Strong and Weak Thermalization of Infinite Nonintegrable Quantum Systems,” *Phys. Rev. Lett.* **106** (2011) no.5, 050405 doi:10.1103/PhysRevLett.106.050405
- [4] Z. H. Sun, J. Cui and H. Fan, “Quantum information scrambling in the presence of weak and strong thermalization,” *Phys. Rev. A* **104** (2021) no.2, 022405 doi:10.1103/PhysRevA.104.022405 [arXiv:2008.01477 [quant-ph]].
- [5] F. Chen, et al, “Observation of Strong and Weak Thermalization in a Superconducting Quantum Processor,” *Phys. Rev. Lett.* **127** (2021) 020602, doi:10.1103/PhysRevLett.127.020602
- [6] C. J. Lin and O. I. Motrunich, “Quasiparticle explanation of the weak-thermalization regime under quench in a nonintegrable quantum spin chain,” *Phys. Rev. A* **95** (2017) no.2, 023621 doi:10.1103/PhysRevA.95.023621 [arXiv:1610.04287 [cond-mat.stat-mech]].
- [7] O. Bohigas, M. J. Giannoni and C. Schmit, “Characterization of chaotic quantum spectra and universality of level fluctuation laws,” *Phys. Rev. Lett.* **52** (1984), 1-4 doi:10.1103/PhysRevLett.52.1
- [8] M. Srednicki, “The approach to thermal equilibrium in quantized chaotic systems,” *Journal of Physics A: Mathematical and General*, (1999) 1163

- [9] I. Dumitriu and A. Edelman, “Matrix models for beta ensembles,” arXiv:math-ph/0206043
- [10] V. Balasubramanian, J. M. Magan and Q. Wu, “Tridiagonalizing random matrices,” *Phys. Rev. D* **107** (2023) no.12, 126001 doi:10.1103/PhysRevD.107.126001 [arXiv:2208.08452 [hep-th]].
- [11] V. Balasubramanian, J. M. Magan and Q. Wu, “Quantum chaos, integrability, and late times in the Krylov basis,” [arXiv:2312.03848 [hep-th]].
- [12] D. E. Parker, X. Cao, A. Avdoshkin, T. Scaffidi and E. Altman, “A Universal Operator Growth Hypothesis,” *Phys. Rev. X* **9** (2019) no.4, 041017 doi:10.1103/PhysRevX.9.041017 [arXiv:1812.08657 [cond-mat.stat-mech]].
- [13] J. L. F. Barbón, E. Rabinovici, R. Shir and R. Sinha, “On The Evolution Of Operator Complexity Beyond Scrambling,” *JHEP* **10** (2019), 264 doi:10.1007/JHEP10(2019)264 [arXiv:1907.05393 [hep-th]].
- [14] V. S. Viswanath and G. Mülle, “The Recursion Method: Application to Many Body Dynamics,” *Lecture Notes in Physics Monographs* (1994), Springer Berlin Heidelberg
- [15] C. Lanczos, “An iteration method for the solution of the eigenvalue problem of linear differential and integral operators,” *J. Res. Natl. Bur. Stand. B* **45** (1950), 255-282 doi:10.6028/jres.045.026
- [16] Work in progress.
- [17] E. Rabinovici, A. Sánchez-Garrido, R. Shir and J. Sonner, “Operator complexity: a journey to the edge of Krylov space,” *JHEP* **06** (2021), 062 doi:10.1007/JHEP06(2021)062 [arXiv:2009.01862 [hep-th]].
- [18] P. Caputa, H. S. Jeong, S. Liu, J. F. Pedraza and L. C. Qu, “Krylov complexity of density matrix operators,” [arXiv:2402.09522 [hep-th]].
- [19] E. Rabinovici, A. Sánchez-Garrido, R. Shir and J. Sonner, “Krylov complexity from integrability to chaos,” *JHEP* **07** (2022), 151 doi:10.1007/JHEP07(2022)151 [arXiv:2207.07701 [hep-th]].
- [20] J. D. Noh, “Operator growth in the transverse-field Ising spin chain with integrability-breaking longitudinal field,” arXiv:2107.08287.
- [21] B. L. Español and D. A. Wisniacki, “Assessing the saturation of Krylov complexity as a measure of chaos,” *Phys. Rev. E* **107** (2023) no.2, 024217 doi:10.1103/PhysRevE.107.024217 [arXiv:2212.06619 [quant-ph]].
- [22] F. B. Trigueros and C. J. Lin, “Krylov complexity of many-body localization: Operator localization in Krylov basis,” *SciPost Phys.* **13** (2022) no.2, 037 doi:10.21468/SciPostPhys.13.2.037 [arXiv:2112.04722 [cond-mat.dis-nn]].
- [23] G. F. Scialchi, A. J. Roncaglia and D. A. Wisniacki, “Integrability to chaos transition through Krylov approach for state evolution,” [arXiv:2309.13427 [quant-ph]].
- [24] E. Rabinovici, A. Sánchez-Garrido, R. Shir and J. Sonner, “Krylov localization and suppression of complexity,” *JHEP* **03** (2022), 211 doi:10.1007/JHEP03(2022)211 [arXiv:2112.12128 [hep-th]].
- [25] L. F. d. Prazeres and T. R. de Oliveira, “Continuous Transition Between Weak and Strong Thermalization using Rigorous Bounds on Equilibration of Isolated Systems,” [arXiv:2310.13392 [quant-ph]].
- [26] A. J. Short and T. C. Farrelly, “Quantum equilibration in finite time,” *New J. Phys.* **14** (2012) no.1, 013063 doi:10.1088/1367-2630/14/1/013063 [arXiv:1110.5759 [quant-ph]].
- [27] V. Balasubramanian, P. Caputa, J. M. Magan and Q. Wu, “Quantum chaos and the complexity of spread of states,” *Phys. Rev. D* **106** (2022) no.4, 046007 doi:10.1103/PhysRevD.106.046007 [arXiv:2202.06957 [hep-th]].
- [28] M. Alishahiha and S. Banerjee, “A universal approach to Krylov state and operator complexities,” *SciPost Phys.* **15** (2023) no.3, 080 doi:10.21468/SciPostPhys.15.3.080 [arXiv:2212.10583 [hep-th]].
- [29] <https://turin.ipm.ir/>.